Propagation of acoustic excitations in a liquid at large wavevectors: a molecular-dynamics study

2008 J. Phys.: Condens. Matter 20 104206

(http://iopscience.iop.org/0953-8984/20/10/104206)

J. Phys.: Condens. Matter **20** (2008) 104206 (9pp) doi:10.1088/0953-8984/20/10/104206

Propagation of acoustic excitations in a liquid at large wavevectors: a molecular-dynamics study

Marco Sampoli[1,2], Ubaldo Bafile[3], Fabrizio Barocchi[2,4], Eleonora Guarini[2,4] and Giovanni Venturi[2]

[1] Dipartimento di Energetica, Università di Firenze, via di S. Marta 3, I-50139 Firenze, Italy
[2] CNR-INFM CRS-Soft c/o Dipartimento di Fisica, Università di Firenze, via G. Sansone 1, I-50019 Sesto Fiorentino, Italy
[3] Consiglio Nazionale delle Ricerche, Istituto dei Sistemi Complessi, via Madonna del Piano 10, I-50019 Sesto Fiorentino, Italy
[4] Dipartimento di Fisica, Università di Firenze, via G. Sansone 1, I-50019 Sesto Fiorentino, Italy

E-mail: ubaldo.bafile@isc.cnr.it

Received 13 July 2007, in final form 28 September 2007
Published 19 February 2008
Online at stacks.iop.org/JPhysCM/20/104206

Abstract

A two-decade development of dedicated high-performance instrumentation at major neutron and synchrotron radiation sources has stimulated significant growth in the number and quality of spectroscopic studies of the collective dynamics of fluids, making Brillouin scattering, in its neutron and x-ray 'versions', a fast growing field of research. However, in contrast with the large amount of work done for wavevector Q lower than the position Q_p of the main peak of the static structure factor $S(Q)$, very little is known about the behaviour of acoustic excitations at much larger Q. We present molecular-dynamics simulation results for the translational part of the dynamic structure factor of the molecular liquid CD_4 up to high Q values ($Q \sim 4Q_p$), analysed through the fitting of the viscoelastic model line shape. The analysis, carried out by applying the concepts described in a recent paper, shows that underdamped sound excitations persist at least up to such high Q values, in agreement with the existence of the *distinct* part of $S(Q)$, with the exception of a restricted interval around Q_p where the collective oscillations become overdamped.

1. Introduction

The microscopic dynamics of fluids is usually described in the language of the van Hove distribution functions [1–3], from which two very useful quantities are defined: the intermediate scattering function $F(Q, t)$, i.e. the autocorrelation function of density fluctuations with wavevector magnitude Q, and its frequency spectrum $S(Q, \omega)$, i.e. the dynamic structure factor. (Due to its macroscopically isotropic behaviour, in a fluid there is no dependence on the direction of the vector $\boldsymbol{Q}$.) $S(Q, \omega)$ is particularly important since, besides being a typical output of computer simulations and the goal of theoretical derivations, it is also closely linked to the scattering intensity revealed in spectroscopic measurements, where $\hbar\omega$ and $\hbar Q$ are identified with the energy and momentum transferred from the probe to the sample in the scattering process.

In this paper we will be specifically concerned with the investigation of collective acoustic excitations, which are well-known to determine the shape of $S(Q, \omega)$ at low and intermediate Q values. The study of sound propagation in the microscopic domain, and of the damping processes that accompany it, has been a typical application of laser sources to $S(Q, \omega)$ determinations through the detection of Brillouin light scattering spectra. However, with a probe wavelength in the range of visible radiation, density fluctuations can only be explored in the limit of very low Q. The fluid is then seen as a continuum and the microscopic discreteness of matter does not come into play, a situation well accounted for by the concepts of hydrodynamics.

There are strong motivations for extending these studies towards much higher Q. Moving away from the limit case of hydrodynamics, the dynamical regime of a fluid evolves

Table 1. Fluids whose collective dynamics has been studied by means of neutron or x-ray inelastic scattering. Labels n and x denote the two techniques.

Years		Rare gases and liquids, mixtures	Molecular gases and liquids	Liquid metals and alloys, metal vapours	Molten salts and oxides, solutions, and other fluids
Until 1990	n	Ne, Ar	H_2, N_2, CD_3OD	Pb, Cs, Rb	LiCl, KCl, RbCl
1991–1995	n	He–Ne	SO_2, CCl_4, D_2, D_2O	Ga, Li, Rb, Rb–(RbBr)	
	x		H_2O		
1996–2000	n		D_2, H_2, D_2O	Rb, Ga, K, Ni, Rb–Sb, K–Cs, Li_4Pb	
	x	He	H_2O, NH_3	Al, Li, Na	
2001–2005	n	He–Ne	CD_4, D_2O	K, Hg, Ga, Na–Sn	$Li(ND_3)_4$
	x	Ne	D_2, H_2, H_2O, HF, $C_3H_8O_3$	Ga, Na, Hg, K, Sn, Si	NaCl, NaI, Al_2O_3, $Li(NH_3)_4$
Since 2006	n		CO_2, DF	Ge, Rb, Bi, Li–Bi, Te	
	x		N_2, O_2, H_2O, CH_3OH	Ti, In, Te	$MgAl_2O_4$

towards that of a discrete collection of individual particles, with a smooth transition ruled by the increase of the product $Q\ell$, where ℓ has to be some characteristic length scale related to the distance between particles [4]. Then, in light scattering experiments, a non-hydrodynamic regime can only be reached by increasing ℓ, thus restricting the investigation to dilute gases [5]. Nevertheless, evidence has been collected during the years of the persistence of sound-like excitations beyond the upper limit of hydrodynamic behaviour in many dense liquids [6–9].

The increasing interest in the study of acoustic excitations at wavelengths comparable with the typical interparticle distances of a dense fluid has prompted continuous efforts aimed at developing instrumentation at neutron and synchrotron radiation sources. Inelastic scattering of neutrons and x-rays have in fact proved to be the most effective and productive tools for $S(Q, \omega)$ measurements, when wide ranges of Q and ω need to be investigated. Since visible-light scattering attains Q values of the order 0.01 nm^{-1}, and conventional neutron scattering hardly applies for $Q < 2$ nm^{-1}, much effort has been spent to extend spectroscopic studies to the previously unexplored Q gap between the two techniques. The denomination 'Brillouin scattering', initially referring to light scattering only, has then become a common label for such experimental methods, whatever probe radiation is applied. Besides neutrons and x-rays, mention is also to be made of the very recently demonstrated Brillouin scattering of ultraviolet radiation [10].

Exploiting technical advances, much experimental work has been done in the last 20 years on the collective dynamics of various fluids, and the field is quite an active one nowadays, as it appears from table 1, where we list systems studied with either neutron or x-ray Brillouin scattering only, warning the reader that such a list might not be exhaustive. In table 1 we omitted all items referring to some particular classes of fluids such as supercooled or confined systems, not to speak of solid amorphous materials such as glasses. An extended list of references to the works quoted in the table can be found in [11].

In all these studies, the analysis of experimental results was performed by fitting to the data a spectral function obtained from a suitable model of the classical $S(Q, \omega)$, appropriately modified to account for detailed-balance asymmetry and instrumental resolution broadening. Usually, both the data and the models are presented in the form of constant-Q frequency spectra, and model fitting is performed separately at each investigated Q value, so that for each fit parameter an experimental Q-dependence is obtained.

The understanding of collective excitations in fluids would clearly benefit from a critical comparison of the results obtained by fitting different models on the same data. Depending on the nature and the thermodynamic state of the fluid, and on the explored Q range, it was often shown in the literature that different expressions of $S(Q, \omega)$ are needed for a satisfactory description of the measured spectra. In the liquid phase, for example, the generalization of the hydrodynamic Rayleigh–Brillouin (RB) triplet line shape has usually been found to account rather well for the low Q situation (say, up to about a few nm^{-1}), while expressions obtained by assuming a viscoelastic-like dynamics often provide good fits when Q approaches Q_p, i.e. the position of the main peak of the static structure factor $S(Q)$. (See section 3 for precise definitions of these model line shapes.)

In fact, other line shapes are also applied as fit functions, but in this paper we will only refer to the two just mentioned models. The main reason for this restriction is the fact that they offer a very good example of a general problem arising in the interpretation of the whole body of experimental findings on the subject, namely, that the comparison of results obtained with different models is hindered by the fact that their formulation and parametrization are not reduced to a common scheme. It turns out, indeed, that these two models are usually written in terms of parameter sets whose correspondence is far from being evident; in particular, this fact has led to the use of a variety of criteria for the determination of the dispersion curve, i.e. the Q-dependence of the acoustic excitation frequency.

In a recent paper [11] we addressed the problem of the lack of a unified scheme for the discussion and comparison of the $S(Q, \omega)$ models most frequently employed in the analysis of Brillouin scattering data. We showed there that all these models can be reformulated in a unified way and that, as a consequence, the excitation frequency can be univocally defined and directly obtained from the fit of any of them. Moreover, a detailed understanding of the shape of the dispersion curve was achieved.

In parallel with the mentioned experimental progress, molecular-dynamics (MD) simulation has also grown in power

due to the impressive increase of computing performance. MD has then become an extremely important tool for investigating microscopic properties, and the dynamics of liquids has long been a prototypical field of application of such a simulation technique.

In conjunction with a neutron scattering experiment on the collective dynamics of dense liquid deuteromethane (CD_4) [12], performed in the Q range between 2 and 15 nm^{-1}, we also carried out MD simulations in a standard *NVE* ensemble of 4000 molecules interacting through the *ab initio* multi-site potential by Tsuzuki *et al* [13]. The chosen thermodynamic state is close to the triple point ($T = 97.7$ K and $n = 16.6$ nm^{-3} are the sample temperature and molecular number density). Both experimental and simulation data reported in [12] were analysed by fitting a hydrodynamic-like Rayleigh–Brillouin triplet line shape. A viscoelastic model was also fitted to experimental data in a later work [14].

The MD simulation, however, also offers the possibility of computing quantities that are not accessed experimentally, such as the three partial dynamic structure factors $S_{\alpha\beta}(Q,\omega)$, where α and β are either C or D for carbon and deuterium atoms. As an example of application of the concepts and formulas discussed in [11], we exploited there this important advantage by focusing on the study of the translational collective dynamics, taking directly $S_{CC}(Q,\omega)$ as input data for our analysis.

Most neutron and x-ray works focus on the Q range between the minimum attainable Q (say, of the order of 0.1 nm^{-1}) and some Q value near Q_p (around 20 nm^{-1}). Conversely, little is known, even in simple liquids, about the behaviour of sound propagation at much larger Q. Apart from energy resolution considerations, this is probably due to the fact that the acoustic excitations quickly lose visibility, with increasing Q, since they give rise to inelastic spectral features discernible by the naked eye in a rather limited low-Q range only. This situation is often referred to as that of overdamped, non-propagating, sound modes. In [11], however, we established rigorous criteria for assessing the existence and the damping properties of such excitations. Here we apply those criteria to the analysis of the centre-of-mass dynamics of CD_4, as obtained from the mentioned MD simulations, over a much more extended Q range than that reported before [11], reaching a value of 67 nm^{-1}, which is nearly four times larger than Q_p. In this paper we report on such a study. In section 2 we recall the basic theoretical tools, while the used fit models are briefly presented in section 3. Section 4 deals with the method used to arrive at a quantitative assessment of the excitation frequencies and damping. Finally, sections 5 and 6 contain a discussion of the obtained results and the conclusions, respectively.

2. Theoretical framework

We will briefly summarize in this section the main results exposed in detail in [11]. The commonly adopted theoretical approach for the description of the density autocorrelation function in a classical fluid is expressed in the language of the memory functions discussed, for example, in [2]. A Langevin-type equation is obtained for the time evolution, at constant Q, of the intermediate scattering function:

$$\ddot{F}(Q,t) + \int_0^t \mathrm{d}t'\, M(Q,t-t')\dot{F}(Q,t') + \langle\omega_Q^2\rangle F(Q,t) = 0, \tag{1}$$

where the dots denote time derivatives, $M(Q,t)$ is the second-order memory function,

$$\langle\omega_Q^2\rangle = \int_{-\infty}^{+\infty} \mathrm{d}\omega\, \omega^2 I(Q,\omega) = \frac{k_B T Q^2}{m S(Q)} \tag{2}$$

is the second frequency moment of the normalized dynamic structure factor $I(Q,\omega) = S(Q,\omega)/S(Q)$, k_B is the Boltzmann constant and m is the mass of the particles [2].

Through the use of Laplace transforms, here denoted by a tilde, (1) can be solved, with initial conditions $F(Q,0) = S(Q)$ and $\dot{F}(Q,0) = 0$, to give

$$\frac{\tilde{F}(Q,z)}{S(Q)} = \left[z + \frac{\langle\omega_Q^2\rangle}{z + \tilde{M}(Q,z)} \right]^{-1}. \tag{3}$$

This solution is exact but somehow formal, since the problem is shifted at the level of the (unknown) memory function, but the theory, by itself, gives no prescriptions for the time dependence of $M(Q,t)$. Nevertheless, something is gained with the use of (3), one of the appealing features of the memory function approach being that very simple expressions of $M(Q,t)$ can produce realistic models for the spectral distribution [2, 11]. This is given by [2]

$$I(Q,\omega) = \frac{1}{\pi} \mathrm{Re}\, \frac{\tilde{F}(Q,\mathrm{i}\omega)}{S(Q)}. \tag{4}$$

A general expression for the spectrum is then obtained as

$$I(Q,\omega) = \frac{1}{\pi} \frac{\langle\omega_Q^2\rangle M'(Q,\omega)}{[\omega^2 - \langle\omega_Q^2\rangle + \omega M''(Q,\omega)]^2 + [\omega M'(Q,\omega)]^2}, \tag{5}$$

where $M'(Q,\omega)$ and $M''(Q,\omega)$ are the real and imaginary part, respectively, of $\tilde{M}(Q,\mathrm{i}\omega)$.

All the typically used models of $I(Q,\omega)$ share the common property that they are derivable from memory functions including a δ-function and/or one or more exponential time decays. In [11] it was shown that in this case (3) can be written in the form $\tilde{F}(Q,z)/S(Q) = V(z)/W(z)$, where V and W are polynomials in the complex variable z (with real, Q-dependent, coefficients) and the degree of W, denoted here by p, is the number of exponential terms in $M(Q,t)$ plus two. At any given Q, if z_j (with $j = \mathrm{A}, \mathrm{B}, \ldots$) are the p solutions of the equation $W(z) = 0$ [11], one can also write

$$\frac{\tilde{F}(Q,z)}{S(Q)} = \sum_j \frac{I_j}{z - z_j}, \tag{6}$$

so that, using (4)

$$I(Q,\omega) = \frac{1}{\pi} \sum_j \frac{-\mathrm{Re}\, I_j\, \mathrm{Re}\, z_j + (\omega - \mathrm{Im}\, z_j)\mathrm{Im}\, I_j}{(\mathrm{Re}\, z_j)^2 + (\omega - \mathrm{Im}\, z_j)^2}, \tag{7}$$

where the (complex) amplitudes I_j can be explicitly calculated. Equation (6) corresponds to an intermediate scattering function $F(Q,t)/F(Q,0) = \sum_j I_j \exp(z_j t)$, and this formula shows that the real part of all the roots z_j must be negative for $F(Q,t)$ to decay to zero at large t. The Q dependence of I_j and z_j has been, and will be in the following, omitted for ease of notation.

At low enough Q, all models of $M(Q,t)$ are found to produce two complex solutions which are conjugate to each other, denoted as $z_{\mathrm{A,B}} = -z_\mathrm{s} \pm \mathrm{i}\omega_\mathrm{s}$ (choosing $\omega_\mathrm{s} > 0$). The corresponding amplitudes, complex conjugated as well, are written as $I_{\mathrm{A,B}} = I_\mathrm{s}(1 \mp \mathrm{i}b_\mathrm{s})$. The remaining $p-2$ roots, labelled with $j = \mathrm{C}, \mathrm{D}, \ldots$, and the corresponding amplitudes are real. The spectrum (7) can then be explicitly written as

$$I(Q,\omega) = \frac{1}{\pi}\left[\sum_{j=\mathrm{C,D...}} \frac{I_j(-z_j)}{\omega^2 + (-z_j)^2}\right] + \frac{1}{\pi} I_\mathrm{s}\left[\frac{z_\mathrm{s} + b_\mathrm{s}(\omega+\omega_\mathrm{s})}{(\omega+\omega_\mathrm{s})^2 + z_\mathrm{s}^2} + \frac{z_\mathrm{s} - b_\mathrm{s}(\omega-\omega_\mathrm{s})}{(\omega-\omega_\mathrm{s})^2 + z_\mathrm{s}^2}\right], \tag{8}$$

where the last two terms define two Lorentzian lines with half width z_s, centred at $\omega = \pm\omega_\mathrm{s}$, and distorted by the presence of the 'asymmetry parameter' b_s. These are the Brillouin lines, that are the spectral signature of the acoustic modes (the subscript s stands for 'sound'). The $p-2$ terms in the sum are also Lorentzian lines, symmetric and centred at $\omega = 0$, having as half widths the negative of the real roots of the equation $W(z) = 0$. It is important to note that the asymmetry of the side lines is required to ensure a finite second frequency moment of $I(Q,\omega)$. The time correlation corresponding to the spectrum (8) has the form

$$\frac{F(Q,t)}{F(Q,0)} = \left[\sum_{j=\mathrm{C,D...}} I_j \exp(z_j t)\right] + 2I_\mathrm{s}\exp(-z_\mathrm{s}t)\frac{\cos(\omega_\mathrm{s}t - \varphi)}{\cos\varphi}, \tag{9}$$

that is the sum of $p-2$ exponentially decaying terms plus one exponentially modulated oscillation with a phase shift given by $\tan\varphi = b_\mathrm{s}$.

We have already remarked that no clue for modelling the memory function is provided by theoretical arguments. There is, however, an exception in the limit case $Q \to 0$, where the linearized-hydrodynamics theory of a fluid continuum leads [1, 15, 16] to the formulation of the Rayleigh–Brillouin expression of $I(Q,\omega)$, which, actually, accounts very well for the observed spectra of dense fluids in the whole Q range typical of light scattering studies. Indeed, such a line shape can be obtained by assuming

$$M(Q,t) = 2\nu Q^2\delta(t) + (\gamma_0 - 1)\langle\omega_0^2\rangle \exp(-\gamma_0 D_\mathrm{T} Q^2 t). \tag{10}$$

Here $\nu = [(4/3)\eta_\mathrm{s} + \eta_\mathrm{b}]/(mn)$ is the kinematic longitudinal viscosity, defined through the shear (η_s) and bulk (η_b) viscosities, $\gamma_0 = c_p/c_v$ is the ratio of the constant-pressure to the constant-volume specific heat, $D_\mathrm{T} = \lambda/(nc_p)$ is the thermal diffusivity, λ is the thermal conductivity, and $\langle\omega_0^2\rangle$ is the $Q \to 0$ limit of $\langle\omega_Q^2\rangle$ obtained from (2) by replacing $S(Q)$ with $S(0) = nk_\mathrm{B}T\chi_\mathrm{s}\gamma_0$ where χ_s is the adiabatic compressibility. If c_s denotes the adiabatic sound velocity, it is easily shown that $\langle\omega_0^2\rangle = c_\mathrm{s}^2 Q^2/\gamma_0$.

Proceeding as outlined above, and noting that (10) implies $p = 3$, one recovers immediately the well-known expression of the RB triplet [1–3, 15]

$$I(Q,\omega) = \frac{1}{\pi}\left[I_\mathrm{h}\frac{z_\mathrm{h}}{\omega^2 + z_\mathrm{h}^2} + I_\mathrm{s}\frac{z_\mathrm{s} + b_\mathrm{s}(\omega+\omega_\mathrm{s})}{(\omega+\omega_\mathrm{s})^2 + z_\mathrm{s}^2} + I_\mathrm{s}\frac{z_\mathrm{s} - b_\mathrm{s}(\omega-\omega_\mathrm{s})}{(\omega-\omega_\mathrm{s})^2 + z_\mathrm{s}^2}\right], \tag{11}$$

where the subscript h, standing for 'heat', is attached to the parameters of the central Lorentzian line that reflects the presence of a thermal contribution to the memory function (10). In particular, z_h is the negative of the real root z_C of the equation $W(z) = 0$ and I_h is the corresponding amplitude. Explicit expressions for I_h, I_s and b_s are given in [11], with $I_\mathrm{h} + 2I_\mathrm{s} = 1$.

The parameters entering (11) have explicit expressions for $Q \to 0$, which can be written as series expansions in powers of Q. To lowest order, one finds $z_\mathrm{h} = D_\mathrm{T}Q^2$, $z_\mathrm{s} = [(\gamma_0 - 1)D_\mathrm{T} + \nu]Q^2/2$, $\omega_\mathrm{s} = c_\mathrm{s}Q$, $I_\mathrm{h} = (1 - 1/\gamma_0)$, $I_\mathrm{s} = 1/(2\gamma_0)$, and $b_\mathrm{s} = [3(\gamma_0 - 1)D_\mathrm{T} + \nu]Q/(2c_\mathrm{s})$. On the other hand, for an arbitrary Q-value, the explicit solution of the equation $W(z) = 0$ is required.

3. Fit models

If applied to the Q range typical of neutron or x-ray scattering, the RB triplet does not provide a suitable description of experimental data. With the actual values of thermodynamic and transport coefficients of real fluids, it turns out that the Q range of existence of two complex roots is much smaller than what is found from the spectra of real systems [11]. Such a failure cannot be an unexpected result, if one remembers that the RB line shape is derived under the hydrodynamic assumption of very-long-wavelength excitations. Nevertheless, it appears natural to construct a model for $I(Q,\omega)$ retaining the same functional expression for $M(Q,t)$, but letting its parameters vary freely with Q. We call this the 'generalized RB triplet' (GRB) model, whose memory function reads

$$M(Q,t) = 2B(Q)\delta(t) + (\gamma(Q) - 1)\langle\omega_Q^2\rangle \exp[-\Gamma_\mathrm{T}(Q)t], \tag{12}$$

where the four parameters are unknown functions of Q, which we imagine to be represented by series expansions with lowest-order terms in agreement with the exact RB theory. Thus, for $Q \to 0$ we have $\gamma(Q) \sim \gamma_0$, $B(Q) \sim \nu Q^2$, $\Gamma_\mathrm{T}(Q) \sim \gamma_0 D_\mathrm{T} Q^2$ and $\langle\omega_Q^2\rangle \sim \langle\omega_0^2\rangle$.

$I(Q,\omega)$ is still given by (11), but z_h, z_s, ω_s, I_h, I_s and b_s will now have a Q-dependence different, in general, from that of linearized hydrodynamics, and to be determined by a best-fit procedure. From the fitted quantities the original parameters of (12) can also be obtained, as shown in [11].

The second model considered here is the so-called viscoelastic model. It should be noted that, actually, different expressions have been used under this denomination. They all can be related to the idea of allowing for a frequency

dependence of thermodynamic or transport coefficients (usually the viscosity, from which the name 'viscoelastic' originally derives). Here we will refer to one of these models only, defined by the memory function [2]

$$M(Q,t) = [\omega_{\mathrm{L}}^2(Q) - \gamma(Q)\langle\omega_Q^2\rangle]\exp[-t/\tau(Q)] + (\gamma(Q)-1)\langle\omega_Q^2\rangle\exp[-\Gamma_{\mathrm{T}}(Q)t], \quad (13)$$

where $\omega_{\mathrm{L}}^2(Q) = \langle\omega_Q^4\rangle/\langle\omega_Q^2\rangle$ and $\langle\omega_Q^4\rangle$ is the fourth frequency moment of $I(Q,\omega)$. Equation (13) differs from (12) for the presence of another exponential term with time constant $\tau(Q)$ replacing the δ-function term of (12). This ensures a finite fourth moment, contrary to what happens in the RB case.

Here too, just as in (12), all parameters are unknown functions of Q except for the $Q \to 0$ behaviour, which is the same as in the GRB case for $\gamma(Q)$, $\Gamma_{\mathrm{T}}(Q)$, and $\langle\omega_Q^2\rangle$. Moreover, $\omega_{\mathrm{L}}^2(Q) \sim c_{\mathrm{L}}^2 Q^2$ where c_{L} is the $Q \to 0$ value of the infinite-frequency sound velocity [1], while $1/\tau(Q)$ goes, for $Q \to 0$, to the limit $1/\tau_0 = (c_{\mathrm{L}}^2 - c_s^2)/\nu$ [2, 11].

If one retraces in this case all the steps that lead to (11), by noting that (13) implies $p = 4$, one immediately arrives at the line shape

$$I(Q,\omega) = \frac{1}{\pi}\left[I_{\mathrm{h}}\frac{z_{\mathrm{h}}}{\omega^2+z_{\mathrm{h}}^2} + I_2\frac{z_2}{\omega^2+z_2^2} + I_{\mathrm{s}}\frac{z_{\mathrm{s}}+b_{\mathrm{s}}(\omega+\omega_{\mathrm{s}})}{(\omega+\omega_{\mathrm{s}})^2+z_{\mathrm{s}}^2} + I_{\mathrm{s}}\frac{z_{\mathrm{s}}-b_{\mathrm{s}}(\omega-\omega_{\mathrm{s}})}{(\omega-\omega_{\mathrm{s}})^2+z_{\mathrm{s}}^2}\right] \quad (14)$$

which has a four-line structure that, compared to (11), has one more central Lorentzian line with amplitude I_2 and a half width z_2 given by the negative of the second real root z_{D} of the equation $W(z) = 0$. All amplitudes can be expressed by formulae analogous to those valid in the GRB case [11].

Equations (11) and (14) display the strong similarity that underlies all spectral shapes deriving from memory functions defined in terms of exponential and/or δ functions. The advantage of such a common formulation is that parameters denoted by the same symbol in both models do have the same physical meaning and the same $Q \to 0$ behaviour, since exact hydrodynamics has to be the common limit of both expressions. Then, by comparison of (11) and (14), one immediately sees that I_2 goes to zero with decreasing Q, as explicitly shown in [11]. However, such a similarity has not been recognized and exploited, since in all the recent literature the viscoelastic model is written in a different way, namely by inserting in (5) the expressions

$$M'(Q,\omega) = \frac{1}{\tau(Q)}X_1(Q,\omega) + \Gamma_{\mathrm{T}}(Q)X_2(Q,\omega),$$
$$M''(Q,\omega) = -\omega[X_1(Q,\omega) + X_2(Q,\omega)],$$

where

$$X_1(Q,\omega) = \frac{[\omega_{\mathrm{L}}^2(Q) - \gamma(Q)\langle\omega_Q^2\rangle]}{\omega^2 + (\frac{1}{\tau(Q)})^2},$$
$$X_2(Q,\omega) = \frac{[(\gamma(Q)-1)\langle\omega_Q^2\rangle]}{\omega^2 + \Gamma_{\mathrm{T}}^2(Q)}$$

and using as fit parameters the coefficients of the memory function (13). This way of formulating the viscoelastic model does not offer a clear view of its line shape and of what it has in common with, and where it differs from, the GRB model. It tends, therefore, to mask the possible existence of a transition from a Q range where a hydrodynamic-like description applies (though outside a true hydrodynamic regime) to a Q range where viscoelasticity may begin to set on. In such a case, following the Q behaviour of fit parameters common to both models is of great help in understanding the dynamics of the acoustic modes. An example of such a situation was shown in [11] and will be recalled in section 5.

4. The dispersion curve

Formulating all fit models in the unified form (6) and using the common parametrization displayed in (8) has another important advantage, because it leads to a full understanding of the dispersion curve of the acoustic excitations [11]. In order to see it clearly, it is useful to establish an analogy between these and the motion of a one-dimensional mechanical damped harmonic oscillator.

If any memory effects were absent, i.e. if $M(Q,t) \propto \delta(t)$, (1) would be formally identical to the equation of motion of such an oscillator, namely $\ddot{x}(t) + 2\mu\dot{x}(t) + \Omega_0^2 x(t) = 0$, where Ω_0 is the characteristic frequency of the system and μ is the friction coefficient. For $\mu < \Omega_0$ the solution is a damped oscillation at the frequency $\omega = \sqrt{\Omega_0^2 - \mu^2}$, which identifies Ω_0 as the frequency of the oscillations when $\mu = 0$. If, however, μ is increased up to and above Ω_0, the system crosses the point of 'critical damping' and enters the 'overdamping' regime, where oscillatory motion no longer takes place. The mathematical similarity between the two phenomena suggests a natural criterion for the definition of the Q range where sound modes have a propagating nature, namely the one corresponding to the 'underdamping' situation, where the equation $W(z) = 0$ has a pair of complex conjugate roots. Moreover, in such a case, the acoustic excitation frequency is identified with the frequency ω_{s} of the oscillating part of $F(Q,t)$.

It would be of little use if the fruitful analogy between mechanical oscillators and acoustic excitations at a given Q were established only in the unphysical case of absence of memory, since, as shown in section 3, realistic models for Brillouin spectra correspond to memory functions that do not simply reduce to a δ-function in time. We showed in [11] that this analogy can indeed be extended to such realistic cases without introducing any approximation, since, for any dynamical situation such that (6) holds with two complex z_js, the dispersion curve obeys the relationship

$$\omega_{\mathrm{s}} = \sqrt{\Omega^2 - z_{\mathrm{s}}^2} \quad (15)$$

where, at each Q, Ω is given by

$$\Omega^2 = \frac{\gamma(Q)\langle\omega_Q^2\rangle}{r(Q)}. \quad (16)$$

In order to clarify the meaning of the function $r(Q)$, we note that (15) has the same square-root form recalled before for a

damped harmonic oscillator. Thus, the mechanical analogy introduced above is indeed extendable to all the models characterized by (6), provided that the 'undamped frequency' Ω of the oscillator is correctly defined. Equation (16) shows that this is possible through the use of $r(Q)$ which acts as a renormalization factor. The role of $r(Q)$ is best appreciated if one writes it as

$$r(Q) = \prod_{j=\mathrm{C,D...}} \frac{z_j}{z_j^{(0)}} \tag{17}$$

which also holds true for all models [11]. The symbol $z_j^{(0)}$ stands for the lowest-order term in the Q power expansion of z_j, so that $\lim_{Q\to 0} r(Q) = 1$. It appears then that the relaxation processes that give rise to the central lines in the spectrum (the non-acoustic modes) also affect in a direct way the propagating excitation frequencies (the sound modes), through the determination of both Ω and z_s.

We also observe that in order to use (15) one needs to know various quantities that are either fitted parameters or functions of them, and that the fit of any model line shape parametrized as in (8) directly provides ω_s itself as well. In other words, (15) is useful not to determine ω_s, but to describe in detail its behaviour as a function of Q. We showed in fact in [11] how, by means of (15), the shape of the whole dispersion curve can be explained as the combination of structural, thermal, and damping effects that can be separately recognized.

From the above observations and the general validity of (15) it follows that the normalized intermediate scattering function (9) can be written as the sum of two terms:

$$\frac{F(Q,t)}{F(Q,0)} = I_{\mathrm{rel}} f_{\mathrm{rel}}(Q,t) + 2I_s f_s(Q,t), \tag{18}$$

where $f_{\mathrm{rel}}(Q,0) = f_s(Q,0) = 1$,

$$I_{\mathrm{rel}} = 1 - 2I_s = \sum_{j=\mathrm{C,D...}} I_j,$$

$f_{\mathrm{rel}}(Q,t)$ is the (thermal and/or structural) relaxation part, and the sound term $f_s(Q,t)$ obeys a damped-oscillator differential equation. Such an equation describes both the under-and the overdamping regime of the acoustic excitation. The latter corresponds to the case where the two complex conjugated roots z_A, z_B of the equation $W(z) = 0$ become real and distinct. In both cases one has $\Omega = \sqrt{z_A z_B}$ and $z_s = -(z_A + z_B)/2$, which shows that z_s can be consistently defined also in the case of overdamped excitations, i.e. where it exceeds Ω. Underdamping occurs, instead, when $\Omega > z_s$, in agreement with the fact that for any two real positive numbers x and y one always has $(x + y)/2 \geqslant \sqrt{xy}$, while for complex conjugate x and y the inequality is reversed. The basic quantities determining the damping state of the acoustic oscillation are thus z_s and Ω.

From the spectral point of view, overdamping is reflected by the absence of Brillouin lines, which change into symmetric Lorentzians of half widths $-z_A$ and $-z_B$, also centred at zero frequency and superimposed onto the quasielastic lines. It is worthwhile to note that the finiteness of the second frequency moment (and in the viscoelastic case of the fourth moment as well) implies that the amplitudes of the various lines cannot be all positive.

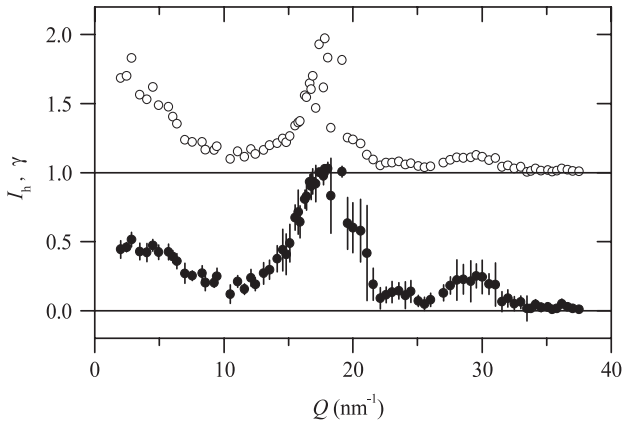

Figure 1. I_h (dots with error bars) and γ (open circles) from the fit of the viscoelastic model including the thermal part (see (13) and (14)).

5. Results

We first recall here the results of the analysis of MD data for CD_4 in the range $2 < Q/\mathrm{nm}^{-1} < 15$, reported in [11]. Least-squares fits of both the generalized Rayleigh–Brillouin and the viscoelastic model were performed. The results are practically indistinguishable at very low Q, as expected, while for Q larger than about 5 nm^{-1} a better agreement with MD data was obtained with the viscoelastic model. The reason for this is that this model permits a more accurate description of the central peak, thanks to the presence of two Lorentzian lines (see (14)), which turn out [11] to have rather different widths. Fitting the GRB model to the same data requires, instead, that we account for such a quasielastic peak with one Lorentzian only, resulting in a lower-quality agreement with the data in the Q range where the intensity I_2 of the second line in the viscoelastic model starts to contribute significantly to the spectral intensity.

Based on these results, we considered it interesting to check whether the viscoelastic model can still provide a valid account of the simulated spectral shape at larger Q. Therefore we extended the same fit procedure to the computed $S_{\mathrm{CC}}(Q,\omega)$ for Q up to 67 nm^{-1}. At all Qs, the fit has been performed in the frequency range defined by the condition that the spectral intensity remain above the value $10^{-3} S_{\mathrm{CC}}(Q,0)$. Figures 1–4 display the main results.

First of all we note (see figure 1) that for Q approaching a value of about 40 nm^{-1}, $\gamma(Q)$ and I_h become very close to unity and to zero, respectively. Considering (13) and (14), both facts mean that the thermal contribution to the dynamics is vanishing. From such Q values on, we have therefore simplified the fit model by deleting the 'heat' mode. The memory function (13) reduces then to a single exponential, and the central peak of the spectrum contains only one Lorentzian contribution. In the following figures, where we display results for the whole studied Q range, it has to be remembered that for $Q > 37.5$ nm^{-1} such a simpler viscoelastic model is applied.

Figure 2(a) shows the fitted static structure factor, which displays the expected behaviour typical of dense fluids. The oscillations around unity, though strongly reduced in amplitude, persist at the highest Q, indicating that *distinct*

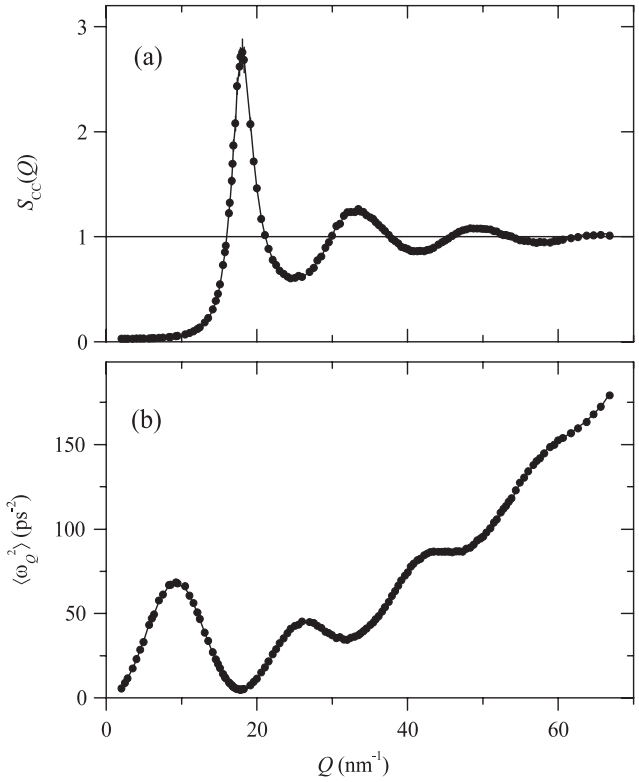

Figure 2. (a) The static structure factor. Fitted values (with error bars smaller than the symbols) are shown as dots. The line is from the frequency integration of the dynamic structure factor. (b) The normalized second frequency moment, evaluated from fitted parameters (dots) and from the theoretical formula (2) (line through the points).

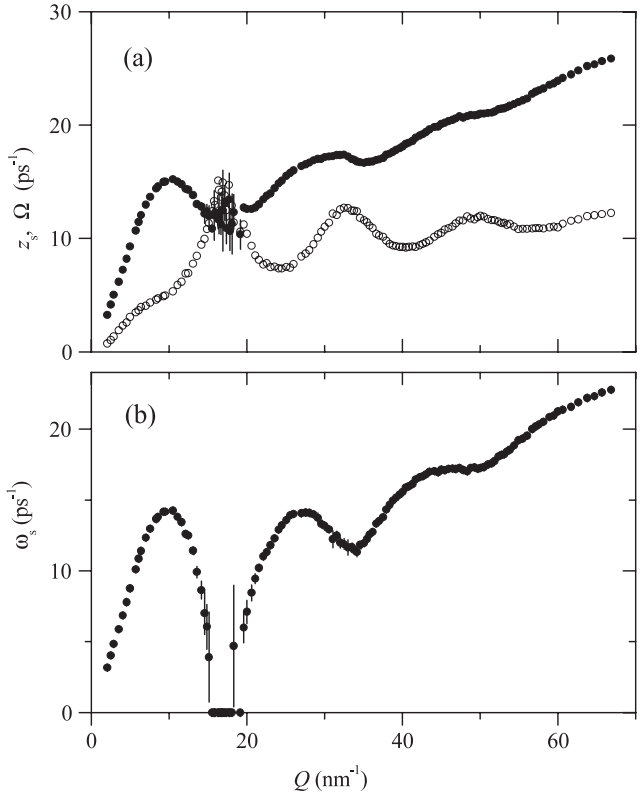

Figure 3. Acoustic excitations. (a) Parameters Ω (dots) and z_s (open circles) of the equivalent damped harmonic oscillator. Error bars of Ω are visible only for $Q \sim Q_p$. Error bars of z_s are comparable in size to those of Ω but are not drawn for the sake of clarity. (b) Dispersion curve (dots with error bars). The zero values around Q_p indicate the vanishing of the propagation frequency ω_s.

intermolecular correlations are still present. The values obtained by direct integration of $S_{CC}(Q, \omega)$ in the whole available frequency range, also shown in figure 2(a), agree very well with the fitted ones. This confirms the very good quality of the fit.

The same kind of agreement with the frequency-integrated evaluation is found for the second frequency moment $\langle\omega_Q^2\rangle$. This again witnesses the goodness of the fit, even more than in the case of $S_{CC}(Q)$, because very high frequencies, which are taken into account in the integration but are not included in the fit range, have a larger weight in the determination of the second than of the zeroth moment. Moreover, in the case of $\langle\omega_Q^2\rangle$, another comparison is possible, namely with the exact theoretical value given by (2). This is shown in figure 2(b), where $\langle\omega_Q^2\rangle$ obtained from the fit parameters (using (22) of [11]) appears to be in excellent agreement with $k_B T Q^2/mS(Q)$, which proves the reliability of our MD spectra at all frequencies and wavevectors. Obviously, the oscillatory behaviour of $\langle\omega_Q^2\rangle$ has opposite phase with respect to that of $S_{CC}(Q)$.

The quantities related to the dispersion curve appear in figure 3. In figure 3(a) we display z_s and Ω, which also feature an oscillating pattern. Ω always stays above z_s, with the exception of a narrow interval around Q_p. Here, Ω is slightly, but systematically, lower than z_s, indicating that a condition of overdamping sets on, with no propagation of the acoustic waves. It also has to be noted that Ω and z_s are

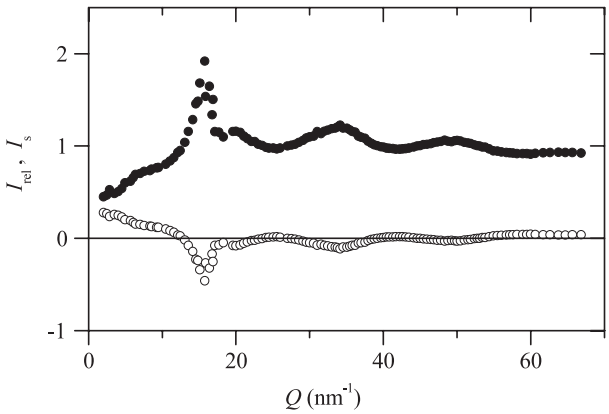

Figure 4. Amplitudes of the relaxational (I_{rel}, dots) and acoustic (I_s, open circles) parts of $F(Q, t)$.

more difficult to determine accurately in this Q range, since the sensitivity of the fit to such parameters clearly decreases when the inelastic (Brillouin) lines move towards $\omega = 0$ and eventually merge with the central Lorentzian line(s) due to the structural and/or thermal relaxation processes. As a result of the Q dependence of Ω and z_s, the dispersion curve plotted in figure 3(b) shows the vanishing of ω_s in the overdamping region. The oscillations of $S_{CC}(Q)$ beyond the first one are

reflected, via (15), (16) and (2), in the behaviour of ω_s, to which evident oscillations of z_s also substantially contribute. In particular, below $Q \simeq 30$ nm^{-1}, ω_s shows a nicely regular shape, somehow resembling the dispersion curve of acoustic phonons in simple crystals. For instance, the first two maxima of ω_s have, to a good accuracy, the same height, although they are related through (15) to quite different pairs of values of Ω and z_s. Whether this has some physical explanation or is just a numerical coincidence we are not able to tell. Further relative maxima of $S_{CC}(Q)$ are not so high as to make the overdamping condition reappear at higher Q, which explains why the acoustic excitations retain a propagative character at all the other Q values investigated here.

Finally, in figure 4 we show the Q dependence of the amplitudes I_{rel} and I_s of (18). I_{rel}, the total intensity of the Lorentzian line(s) in the quasielastic peak, follows the oscillations of $S_{CC}(Q)$, while I_s obviously has an opposite phase due to the complementarity condition $I_{rel} + 2I_s = 1$. For Q larger than Q_p both quantities quite quickly approach the values one and zero, respectively, indicating the weakening of the sound excitations, which, however, are still present in the whole Q range.

6. Conclusions

The critical review, carried out in [11], of current methods for the analysis and the interpretation of collective-dynamics spectra has led us to a rigorous definition of the quantities that determine the properties of acoustic oscillations in fluids. This approach has been applied here to the investigation of such excitations in a wavevector range scarcely studied so far, because of the widely spread assumption that the dynamic structure factor of fluids does not, actually, show the presence of any feature that can be evidently related to sound modes. On the contrary, using MD data for the translational dynamics of the simple molecular liquid deuteromethane, we have shown here that such excitations exist and possess a propagative character. However, their contribution to the total scattering is strongly reduced with increasing Q, as the intensity associated with the sound modes decays to zero following an oscillatory pattern quite similar to that related to *distinct* correlations in the static structure factor.

We have also shown that for Q values around Q_p the sound oscillations cross the transition from the under- to the overdamped regime. This is mainly due to the strong decrease of the renormalized 'undamped' frequency Ω, driven by the presence of a high peak in $S_{CC}(Q)$. Although the latter is a typical feature of dense insulating liquids, however, it cannot be stated that such an overdamping should generally occur. Indeed, even in the case of so highly structured a fluid as liquid methane, the overdamping condition seems to be a rather 'weak' one, the dynamical behaviour being very close to a 'critical damping' situation, with Ω only slightly smaller than the damping parameter z_s. Not surprisingly, all subsequent peaks of $S_{CC}(Q)$ are not able to produce again such a situation. Thus, the existence of propagative sound modes at large Q appears to be limited by the decay of their intensity rather than by the vanishing of their frequency.

The disappearance of propagation in a rather restricted Q range has never been reported so far for molecular liquids, though it was predicted by a kinetic-theoretical approach [17] in a hard-sphere system and found in a GRB analysis of a simulated Lennard-Jones dense fluid [18] and of neutron data on liquid argon [9]. However, we believe that a deeper understanding of this dynamical phenomenon is obtained if one interprets it, as done here, in terms of the damping state variation of an equivalent harmonic oscillator, recognizing the fundamental role of the quantities Ω and z_s. It should be noted that, in this respect too, the dynamic centre-of-mass behaviour of fluid methane closely resembles that of monatomic insulating liquids, as already pointed out in [12].

Another main result of this work is that the concept of viscoelasticity, as implemented in (13), can account very accurately for the translational dynamics of simple liquids in a very wide Q range. On the other hand, we have also shown that the density fluctuations of thermal origin slowly lose importance while Q is increased, though displaying oscillations in phase with those of the dispersion curve. In the present case, the second term of (13) already ceases to contribute to the memory function at Q of the order of $2Q_p$.

Indeed, all the quantities shown in the figures, as well as other parameters not reported here, appear to reflect directly the oscillatory behaviour of $S_{CC}(Q)$. This suggests that structural properties have a strong relationship with the whole dynamics and, in particular, that a direct link exists between the presence of collective excitations of acoustic character and that of structural correlations beyond the pure *self* (i.e. single-molecule) ones. Such a relationship is obviously well established at low Q, but, to our knowledge, was not evidenced before in Q ranges above the main peak of the static structure factor.

In conclusion, we have provided a detailed and consistent picture, in a wide Q range, of the collective dynamics of deuterated methane as obtained from accurate MD simulations carried out with a realistic *ab initio* interaction potential. The methods applied here are of general validity and applicable to a variety of fluids. This result should stress the importance of performing careful experimental determinations in as wide as possible Q and ω ranges, in order to validate simulation results that can give precious insight into unexplorable Q and ω ranges or into experimentally inaccessible properties of real fluids.

Acknowledgments

We acknowledge fruitful discussions with M Celli, D Colognesi, and L Ulivi.

References

[1] Boon J P and Yip S 1980 *Molecular Hydrodynamics* (New York: McGraw-Hill)
[2] Balucani U and Zoppi M 1994 *Dynamics of the Liquid State* (Oxford: Clarendon)
[3] Hansen J P and McDonald I R 1986 *Theory of Simple Liquids* 2nd edn (London: Academic)
[4] Bafile U, Verkerk P, Barocchi F, de Graaf L A, Suck J-B and Mutka H 1990 *Phys. Rev. Lett.* **65** 2394

[5] Clark N A 1975 *Phys. Rev.* A **12** 232
Ghaem-Maghami V and May A D 1980 *Phys. Rev.* A **22** 698
Letamendia L, Chabrat J P, Nouchi G, Rouch J, Vaucamps C and Chen S-H 1981 *Phys. Rev.* A **24** 1574
Letamendia L, Joubert P, Chabrat J P, Rouch J, Vaucamps C, Boley C D, Yip S and Chen S-H 1982 *Phys. Rev.* A **25** 481
[6] Scopigno T, Ruocco G and Sette F 2005 *Rev. Mod. Phys.* **77** 881
[7] Hosokawa S, Greif J, Demmel F and Pilgrim W-C 2003 *Chem. Phys.* **292** 253
Hosokawa S, Sinn H, Hensel F, Alatas A, Alp E E and Pilgrim W-C 2002 *J. Non-Cryst. Solids* **312–314** 163
[8] Bove L E, Sacchetti F, Petrillo C, Dorner B, Formisano F and Barocchi F 2001 *Phys. Rev. Lett.* **87** 215504
[9] de Schepper I M, Verkerk P, van Well A A and de Graaf L A 1983 *Phys. Rev. Lett.* **50** 974
[10] Masciovecchio C, Gessini A and Santucci S C 2006 *J. Non-Cryst. Solids* **352** 5126
[11] Bafile U, Guarini E and Barocchi F 2006 *Phys. Rev.* E **73** 061203
[12] Guarini E, Bafile U, Barocchi F, Demmel F, Formisano F, Sampoli M and Venturi G 2005 *Europhys. Lett.* **72** 969
[13] Tsuzuki S, Uchimaru T and Tanabe K 1998 *Chem. Phys. Lett.* **287** 327
[14] Bafile U, Barocchi F, Demmel F, Formisano F, Guarini E, Sampoli M and Venturi G 2006 *J. Neutr. Res.* **14** 281
[15] Berne B J and Pecora R 1976 *Dynamic Light Scattering* (New York: Wiley) chapter 10
[16] Mountain R D 1966 *Rev. Mod. Phys.* **38** 205
[17] de Schepper I M and Cohen E G D 1980 *Phys. Rev.* A **22** 287
[18] de Schepper I M, van Rijs J C, van Well A A, Verkerk P, de Graaf L A and Bruin C 1984 *Phys. Rev.* A **29** 1602